

DINOV2-Assisted Selection and Life Cycle Cost Control of Green Building Textiles

Hangtian Liu

How to cite: Liu H. DINOV2-Assisted Selection and Life Cycle Cost Control of Green Building Textiles. Textile & Leather Review. 2026; 9:828-848. <https://doi.org/10.31881/TLR.2026.828>

How to link: <https://doi.org/10.31881/TLR.2026.828>

Published: 31 March 2026



DINOV2-Assisted Selection and Life Cycle Cost Control of Green Building Textiles

Hangtian Liu

Taiyuan City Vocational and Technical College, Taiyuan 030009, Shanxi, China

LLTTTT2570@163.com

Article

<https://doi.org/10.31881/TLR.2026.828>

Received 30 July 2025; Accepted 24 September 2025; Published 31 March 2026

ABSTRACT

The lack of selection accuracy and poor life cycle cost control of functional textile materials in green buildings restricts their performance in energy savings, safety, environmental protection, and other performance indicators. This paper implements a method for intelligent selection and life cycle cost control of building textile materials that integrates the DINOV2 model. First, a local texture feature extraction module is introduced into DINOV2 to enhance its modeling capabilities for high-frequency textures and complex tissue structures, enabling image-level semantic recognition of the sustainable performance of textile materials. Subsequently, a multi-factor regression model is constructed to quantify the comprehensive cost of textile materials by combining functional parameters such as material heat and moisture regulation, flame retardancy, durability, and economic data. Finally, an adaptive mutation rate mechanism is introduced into the genetic algorithm (GA) to perform multi-objective optimization on material combinations that meet the performance constraints of green buildings. Experimental results show that the proposed method can complete optimization in 63.1 seconds for the selection of 80 types of textile materials, achieving the lowest life cycle cost of 295,000 CNY and a performance score of 94, providing an effective solution for the selection of textile materials and full life cycle cost control in green buildings.

KEYWORDS

green building, textile material selection, full life cycle cost control, DINOV2 model

INTRODUCTION

The rapid development of green buildings has raised the requirements for environmental protection, functionality, and sustainability of interior decoration materials, promoting the widespread application of building

textile materials in thermal insulation, sound absorption, flame retardancy, and other aspects [1,2]. Functional textiles play a key role in wall decoration, sound insulation, and other areas due to their lightweight, flexibility, and multifunctionality [3,4]. However, in green building projects, the selection of textile materials still mainly relies on experiential judgment and traditional performance indicators, lacking a multidimensional evaluation system based on structural texture, functional finishing, and actual use environment, which makes efficient and accurate material matching difficult.

Existing research focuses on the selection and life cycle assessment of hard materials, while image feature extraction and intelligent recognition of textile materials remain relatively weak. Traditional methods have issues such as poor generalization and blurred edges when processing fabric images with high-frequency textures and complex structures, affecting classification effectiveness [5-7]. Indicators such as carbon emissions and renewability of textile materials in green buildings have not yet been systematically expressed, and life cycle cost assessments are mostly at the initial procurement level, ignoring factors such as maintenance and replacement. It is difficult to balance functionality and economy, and to adapt to diverse material types and application requirements.

This paper proposes a method for intelligent selection and full life cycle cost control of green building textile materials that integrates the DINOv2 visual model. Based on the self-supervised Transformer structure, DINOv2 can generate high-quality texture representations under unlabeled conditions, which is suitable for image feature extraction of materials with complex textures. Through the local texture extraction mechanism, structure recognition and classification of multiple types of building textile materials are realized, and the life cycle cost regression model is constructed by combining their performance parameters and economic data to quantify costs at each stage. In the optimization stage, an adaptive mutation genetic algorithm is introduced to achieve multi-objective trade-offs in material combinations, improving the performance-cost matching of the selected materials and providing a new path for the intelligent application of green building materials.

RELATED WORKS

In recent years, with the in-depth development of the green building concept, the application scenarios of textile materials in buildings have continuously expanded, extending from initial soft decoration to functional

fields such as shading systems and acoustic control [8-10]. Functional architectural textiles are playing an increasingly important role in green buildings due to their lightweight, strong structural flexibility, and ease of construction and replacement [11,12]. At the same time, green buildings have raised the requirements for sustainable performance of materials, such as renewability, low carbon emissions, and environmental friendliness, prompting researchers to pay attention to the ecological performance and resource efficiency of textile materials throughout their life cycle.

The performance evaluation and cost control of green building materials have always been core issues in building sustainability research. With the development of computer vision and machine learning technology, more studies have attempted to introduce image recognition, feature extraction, and other methods into the process of building material selection and life cycle analysis [13,14]. Among these, the application of building textile materials in green building envelope systems has gradually increased, making it particularly important to accurately predict and optimize their comprehensive performance throughout the life cycle.

In terms of material identification, traditional methods mostly rely on physical testing and manual coding, which present problems such as low efficiency and strong subjectivity. Recently, the Transformer structure has performed well in image understanding tasks [15]. As a new development in unsupervised visual representation learning, DINOv2 has demonstrated strong generalization ability in image encoding and semantic feature extraction of textured building materials. Some studies have applied it to material classification and defect detection tasks, but its use in life cycle cost modeling is still at the exploratory stage.

In the field of life cycle cost estimation, mainstream methods often rely on static parameters and manual model construction [16,17]. Current research is insufficient in dealing with complex high-dimensional inputs and heterogeneous data fusion [18,19]. To improve the accuracy and automation level of cost prediction, some scholars have combined machine learning to predict building material energy consumption, operation and maintenance expenses, or environmental impact [20]. In addition, existing optimization methods mostly rely on static weight configuration or fixed evolution strategies, which are difficult to adapt to the actual needs of multi-constraint, nonlinear, and dynamic decision-making in green building projects.

In response to the above challenges, this paper implements a method for identifying and controlling the cost of building textile materials throughout the life cycle based on DINOv2, aiming to improve the scientificity

and economic controllability of textile material selection in green buildings, and promote the efficient integrated application of functional textiles in the construction field.

TEXTILE MATERIAL IDENTIFICATION AND SELECTION BASED ON DINOv2 MODEL

Multi-Scale Feature Extraction Method Integrating Environmental Protection Characteristics

While DINOv2 excels at general image representation through self-supervised learning, its global attention mechanism remains limited when processing architectural textiles with high-frequency textures and large microstructural variations. Detailed features such as weave density, fiber orientation, and local texture repetitiveness are smoothed or ignored by the global attention mechanism, resulting in insufficient fine-grained semantic recognition capabilities. To improve the model's ability to represent complex texture structures in architectural textile material images and construct high-quality feature representations suitable for type identification and feature calibration, this paper introduces a local texture feature extraction module in the DINOv2 structure. This module integrates multi-scale convolutional perception units, local area encoding mechanisms, and window-level feature fusion strategies to form a complete local texture modeling path. The module embedding position is set before the Transformer encoding layer to enhance the texture expression ability of the original image input.

The input image I first passes through an initial feature extractor consisting of a stack of L_c convolutional layers to obtain the basic texture response map F_0 , which is expressed as:

$$F_0 = \text{Conv}_{L_c}(I) \quad (1)$$

The convolution group uses a fixed receptive field, the same stride length, and padding method to ensure continuous retention of basic texture information in the spatial domain. The feature map output at this stage is divided into non-overlapping windows of equal size. Each window corresponds to a local area in the architectural textile material image, retaining microscopic information such as weave density, arrangement direction, and structural edges in the area.

In each window, a local self-attention mechanism is introduced to achieve feature aggregation by calculating

the similarity between any two pixel vectors in the window. Let the feature tensor in the window be represented as X_i , then its attention output is expressed as:

$$Z_i = \text{Softmax} \left(\frac{Q_i K_i^T}{\sqrt{d}} \right) V_i \quad (2)$$

$$Q_i = X_i W^Q \quad (3)$$

$$K_i = X_i W^K \quad (4)$$

$$V_i = X_i W^V \quad (5)$$

where W^Q , W^K , W^V are learnable linear transformation matrices.

To solve the problem of texture segmentation between windows, a window translation strategy is introduced to adjust the starting position of window division between adjacent modules so that texture areas at different positions can be staggered. The features extracted by multiple sets of sliding windows are integrated, and the stable output of local texture features is completed through linear mapping, normalization, and residual connection.

Figure 1 shows the visual effect of the window division and translation mechanism in the process of local texture modeling. The right figure implements window staggered sampling based on the edge response map, which improves the model's ability to express texture continuity.



Figure 1. Schematic diagram of window division and texture enhancement of textile images

The image features output by the backbone encoder are divided into two parts: one part enters the material discrimination branch, supervising the classification of building textile material types through the fully connected layer and the Softmax classifier and outputting the material category recognition result; the other part forms a semantic feature vector after global pooling, which is used in combination with the functional parameters and economic data of the material as a unified input for life cycle cost modeling.

Full Life Cycle Economic Model Including Carbon Cost

The life cycle cost model of building textile materials takes image feature vectors, functional parameters, and economic indicators as inputs and constructs a multivariate regression framework to evaluate full life cycle cost performance. Image features are generated by the DINOv2 local texture extraction module, reflecting material texture complexity and structural distribution; functional properties include thermal resistance, sound absorption, flame retardancy, weather resistance, etc.; economic properties include initial cost, maintenance frequency, energy consumption, and carbon footprint. The relevant data comes from the public building materials platform and manufacturer technical parameters, which are unified, standardized, and merged into the model input matrix. The output is the total life cycle cost of the material per unit area, covering expenditures such as procurement, maintenance, replacement, energy consumption, and recycling. The discounted value is calculated using a fixed discount rate.

The regression modeling adopts a regularized multivariate linear regression structure, and the objective function introduces an L2 regularization term to suppress the multicollinearity problem of high-dimensional features and prevent parameter overfitting:

$$L(\mathbf{w}, b) = \frac{1}{n} \sum_{i=1}^n (y_i - \hat{y}_i)^2 + \lambda \|\mathbf{w}\|_2^2 \quad (6)$$

where \mathbf{w} is the regression weight vector, b is the bias term, and λ is the regularization coefficient.

The weight coefficient learning process aims to minimize the mean square error between the actual life cycle cost and the model prediction cost, using the batch gradient descent method to update parameters.

The feature importance evaluation is based on the normalized value ranking of the regression coefficients. The results are used to judge the influence of different textile material parameters on the total life cycle cost and provide a weight reference for subsequent selection optimization. The model architecture supports the expansion of input feature dimensions, which is convenient for introducing other material properties or environmental factors later, and has strong versatility.

In the output structure design, the model provides a single material cost valuation result and connects to the genetic algorithm optimization framework in the form of a matrix in the subsequent module, used as an objective function evaluation indicator to connect the three-stage technical path of identification, prediction, and optimization. The model structure and data input interface are encapsulated as a unified call module, integrated into the material selection platform, and realize the automatic update of parameter configuration and prediction results. Figure 2 shows the overall architecture and data flow process of the model.

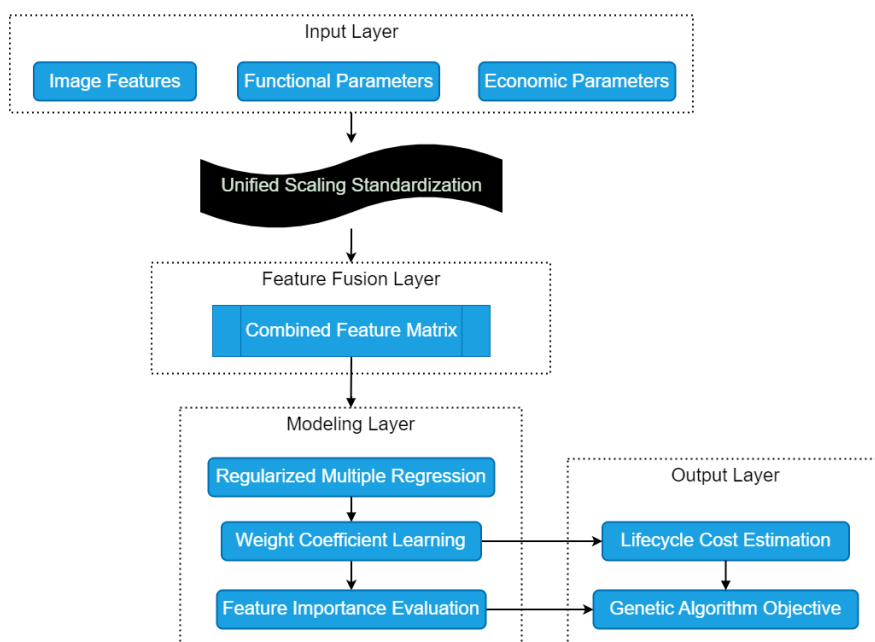


Figure 2. Framework of the life cycle cost prediction model for building textile materials

Multi-Objective Optimization Algorithm for Green Constraints

The selection optimization process of building textile materials is based on the genetic algorithm structure. By introducing an adaptive mutation rate mechanism to adjust the population evolution strategy, the optimal

balance solution between life cycle cost and performance parameters is searched in the solution space. The optimization objective function is based on the predicted value of the textile material life cycle cost output by the previous module, and the multi-objective weight function is set in combination with the functional constraints of the material to dynamically evaluate the comprehensive advantages and disadvantages of each candidate solution during the evolution process. The optimization objective function is expressed as:

$$F(\mathbf{m}) = \omega_c \cdot C_{\text{total}}(\mathbf{m}) + \omega_s \cdot (1 - S(\mathbf{m})) \quad (7)$$

where \mathbf{m} represents the candidate material combination, $C_{\text{total}}(\mathbf{m})$ is the total life cycle cost per unit area, $S(\mathbf{m})$ is the performance satisfaction score of the combination, and ω_c and ω_s represent the weight coefficients of cost and performance, respectively. $S(\mathbf{m})$ integrates key functional indicators such as thermal and moisture regulation, flame retardancy, and durability, with values ranging from 0 to 1. This score first compares the actual value of each performance parameter with the project's preset design threshold and normalizes it into a single satisfaction score. It then assigns different weights to each performance indicator based on its relative importance within the specific green building project and performs a weighted aggregation. The closer the resulting $S(\mathbf{m})$ score is to 1, the more comprehensively the material combination's overall performance meets the design requirements.

The candidate material combination encoding is constructed in the initialization stage, and each individual gene fragment represents a type of optional textile material. The encoding adopts a fixed-length integer string structure:

$$\mathbf{g} = [g_1, g_2, \dots, g_n], \quad g_i \in \{1, 2, \dots, K\} \quad (8)$$

where g_i represents the material number corresponding to the i -type building component, n represents the number of different types of components for which textile materials need to be selected, K is the total number of optional textile materials in the candidate material library, and the population size is set to 100. The first generation of individuals is randomly generated from the candidate textile material library selected by the recognition module, and all meet the minimum functional coverage constraints, including technical

indicators such as thermal performance, acoustic performance, fire resistance, and environmental adaptability.

The fitness function is composed of the total life cycle cost per unit area and functional satisfaction. The weight distribution is set according to the actual project priority. In scenarios where material cost control is prioritized, the influence weight of economic factors is increased, and in scenarios where functional constraints are strict, the proportion of material performance matching evaluation is increased. After the population fitness is standardized, it enters the selection stage, and the tournament selection mechanism is used to increase the probability of retaining high-quality individuals.

The crossover operation uses a two-point crossover method to achieve the interchange of candidate material combinations. The crossover probability is set to 0.9. The adaptive mutation rate mechanism is applied to the mutation operation link. A higher mutation probability is set in the early stage of population evolution, and the mutation probability is automatically reduced in the population convergence stage. The mutation rate is dynamically adjusted with the number of iterations:

$$p_m(t) = p_{\max} - \left(\frac{t}{T_{\max}}\right) \cdot (p_{\max} - p_{\min}) \quad (9)$$

where t is the current generation, T_{\max} is the maximum iteration generation, p_{\max} and p_{\min} are the maximum and minimum mutation rates, respectively.

This mutation rate strategy works in conjunction with the optimization objective function to achieve the algorithm's phased optimization goals. In the early stages of evolution, a higher mutation rate helps maintain population diversity, promotes global exploration, and achieves early cost control. As iterations progress, the mutation rate gradually decreases, and the algorithm's strategy shifts from exploration to exploitation. At this point, the population has converged to a high-performance region, and a lower mutation rate facilitates fine-tuning of high-performing individuals, allowing for a focus on improving performance satisfaction scores in the later stages. As shown in the optimization results in Section "Optimized Material Selection and Cost Control Effect", in the performance-oriented Option 5 (Option-5), this method successfully improved performance satisfaction to 94 points while keeping life cycle cost at a minimum of 295,000 CNY, significantly out-

performing the comparison algorithm. This validates the effectiveness of the subsequent refined search. Furthermore, this adaptive strategy enabled the algorithm to converge quickly in 63.1 seconds when processing 80 materials, demonstrating its excellent computational efficiency while maintaining high accuracy.

The mutation operation randomly perturbs the material index site within the individual, re-extracts the material category that meets the current constraints in the candidate material library to replace the original gene fragment, and ensures the feasibility of the solution after mutation.

Individual updates adopt an elite retention strategy, directly passing the individuals with the highest fitness in the previous generation to the next generation to avoid the loss of optimal solutions. The iteration termination condition is based on the convergence threshold of the fitness function. If the optimal fitness of the population is not improved by the set amplitude for 20 consecutive generations, the evolution process is terminated. At the same time, the maximum iteration round is set to 200 to limit the operation time. The final output textile material combination is the solution with the lowest life cycle cost under the performance constraint.

EXPERIMENTAL DESIGN AND CONFIGURATION

Dataset and Experimental Environment

The experiment uses a dataset of architectural textile material images, which are sourced from public textile material libraries, green building design cases, and field-collected images. To ensure data quality, all images underwent a rigorous data cleaning process: blurry, heavily occluded, or mislabeled samples were removed. Subsequently, uniform preprocessing was performed: the resolution was cropped and resized to 256×256 pixels using bilinear interpolation, and pixel values were normalized to the range $[0, 1]$. Data augmentation included random horizontal flipping, $\pm 15\%$ brightness perturbation, and Gaussian noise overlay to increase model robustness. Texture annotation was performed using a semi-automatic tool and cross-validated by two domain experts to ensure consistency. The final dataset covers 12 common materials, with at least 500 images for each. Stratified random sampling was used to partition the dataset, strictly splitting each class into training and validation sets in an 8:2 ratio. This ensures balanced class distribution and independence of the partitioning process, preventing data leakage.

To improve the model's perception of material sustainability, environmental label information corresponding

to each type of material is introduced into the dataset, and the applicable climate zone category is marked according to the collection source, which is used to assist the environmental adaptability analysis in full life cycle cost modeling.

The experimental platform uses an NVIDIA GeForce RTX 4070 GPU (12 GB video memory), the host is equipped with an AMD Ryzen 7 5800X processor, 64 GB DDR4 memory, and the operating system is Windows 11. Model training and evaluation rely on the PyTorch 2.0.1 framework, CUDA version 11.8, and the image preprocessing and visualization module is based on OpenCV 4.8.0 and Matplotlib 3.7.2.

DINOv2 Model Training and Optimization Process

The backbone model uses the DINOv2 ViT-B/14 structure, the parameters are initialized using the Meta official pre-trained weights, and the input image size is set to 224×224 . The local texture enhancement module is embedded before the backbone encoder, which contains two layers of 3×3 convolution, ReLU activation, and BatchNorm normalization structure. The output features are divided into 64×64 windows in the spatial dimension, and local modeling is performed through a fixed-step sliding window operation. A multi-head self-attention mechanism is introduced in the window, with the dimension set to 256 and the number of heads to 4. Linear mapping is performed after the local similarity weights are fused. After the global feature output is encoded by the trunk Transformer module, the branch outputs the material category prediction vector and the global semantic embedding representation. The loss function uses a combination of cross-entropy loss and an L2 regularization term; the optimizer uses AdamW, the initial learning rate is set to 5×10^{-4} , the batch size is 64, the number of training rounds is 100, and the learning rate scheduler uses the cosine annealing strategy. The training set and validation set are divided in a ratio of 8:2, and the division method maintains a balanced distribution of each type of image. A structural jitter strategy with a DropPath rate of 0.1 is added during the weight update process to avoid model overfitting.

TEXTILE MATERIAL SELECTION AND COST CONTROL OPTIMIZATION RESULTS

Textile Material Identification and Classification Results

To systematically evaluate the classification performance of the visual model in the sunshade material image recognition task, the experiment constructed a dataset of five representative types of materials selected from

the main dataset: glass fiber cloth, coated fabric, sunshade net, geotextile, and membrane material. Each type contains 500 image samples, resulting in a total of 2,500 images for this comparative analysis. Based on this, a comparative analysis was conducted between the original DINOv2 ViT-B/14 model and DINOv2 with the improved mechanism. Confusion matrices between the predicted and true labels were constructed for both models. The original model was initialized using official pre-trained weights and subsequently fine-tuned on the textile materials dataset. All training hyperparameters remained consistent across the two models. The results are shown in Figure 3.

		Baseline DINOv2					Improved DINOv2					
True	Glass Fiber	83	2	4	5	6	Glass Fiber	96	2	0	1	1
	Coated Fabric	7	81	0	4	8	Coated Fabric	3	89	1	4	3
	Shade Net	4	2	81	7	6	Shade Net	2	0	96	1	1
	Geotextile	5	1	4	83	7	Geotextile	0	2	1	96	1
	Membrane	4	7	8	3	78	Membrane	3	2	5	0	90
		Glass Fiber	Coated Fabric	Shade Net	Geotextile	Membrane	Glass Fiber	Coated Fabric	Shade Net	Geotextile	Membrane	
		Predicted					Predicted					

Figure 3. Comparison of textile material recognition and classification results

The correct prediction values on the diagonal of the baseline model are concentrated between 78 and 83; the improved model is concentrated between 89 and 96, and misclassification is reduced. The reason for the above performance difference is that the optimization of the model structure introduces more effective feature representation capabilities. As the original DINOv2 structure, the baseline model has strong global representation extraction capability, but it still has deficiencies in capturing local texture or edge features, which can easily cause confusion between similar areas of materials. The improved model integrates a multi-scale attention mechanism and therefore has advantages in category boundary clarity and discriminative information extraction.

Effect of Life Cycle Cost Prediction

To verify the effectiveness of the model in the life cycle cost estimation task, the experiment was compared with the gradient boosting tree model (XGBoost) and the widely used support vector regression (SVR). The

experiment compared the error distribution and fitting trend between the model prediction value and the true value through 100 groups of samples, and analyzed its performance in terms of accuracy, stability, and deviation control. Figure 4 shows the prediction of life cycle cost by each method.

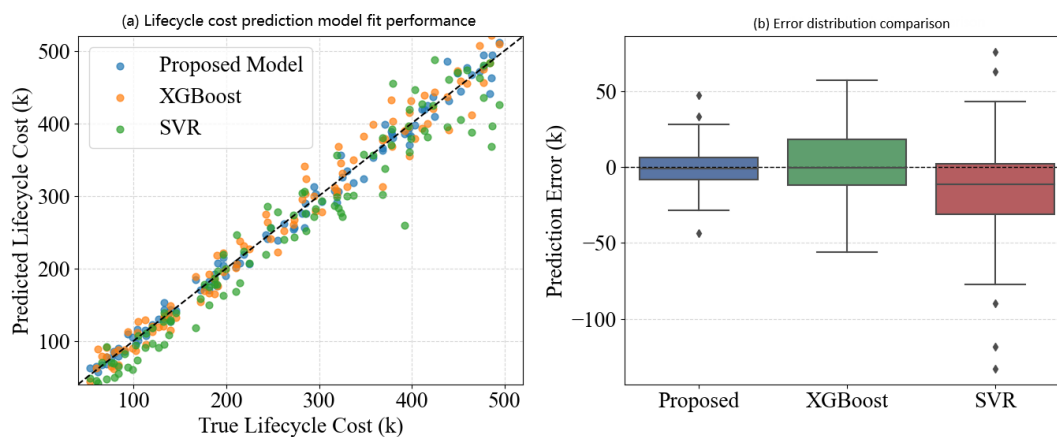


Figure 4. Comparison of fitting effect and error distribution of life cycle cost prediction models

As seen in Figure 4(a), most of the prediction points of the proposed model are concentrated, followed by XGBoost, while the scatter distribution of SVR is relatively dispersed, with a significant trend of deviation from the diagonal line. Figure 4(b) shows the prediction error. The median error of the proposed model is close to 0, and the box range is the smallest. The error range of XGBoost is slightly larger but still relatively concentrated; while the error distribution of the SVR model is the widest, and there are more outliers in the negative direction. From the perspective of model mechanism, the model in this paper integrates feature selection, integration strategy, and regularization regulation, so it demonstrates good robustness and generalization ability in modeling the complex nonlinear relationship of life cycle cost. Although XGBoost has gradient iterative optimization and loss control mechanisms and can capture some nonlinear features, it is limited by the depth of tree structure and sample sensitivity, and the prediction results fluctuate slightly. SVR relies on kernel functions to construct feature maps. Although it has certain nonlinear fitting capabilities, it is more likely to deviate under high variance samples and wide-range inputs, and errors are prone to accumulation and deviation.

To evaluate the robustness and applicability of the life cycle cost prediction model under different carbon

price scenarios, this experiment conducted a systematic error analysis on the material cost data under five carbon price conditions, from low to high. The results are shown in Table 1.

Table 1. Life cycle cost prediction error and significance under carbon price fluctuations

Carbon Price (CNY/ton CO ₂)	Proposed Model MAE (×10 ⁴ CNY)	XGBoost MAE (×10 ⁴ CNY)	SVR MAE (CNY)	(×10 ⁴ p-value vs XGBoost)	(Proposed p-value (Proposed vs SVR))
50	1.25	1.43	1.58	<0.05	<0.05
100	1.30	1.48	1.65	<0.05	<0.05
150	1.35	1.55	1.70	<0.05	<0.05
200	1.40	1.60	1.78	<0.05	<0.05
250	1.45	1.65	1.85	<0.05	<0.05

Table 1 shows the comparison of the life cycle cost prediction errors of the proposed model, XGBoost, and SVR models under different carbon price conditions. As the carbon price increases, the errors of the three models increase slightly, but the proposed model always maintains the lowest Mean Absolute Error (MAE), ranging from 12,500 CNY to 14,500 CNY, which is better than XGBoost and SVR. The p-values are all less than 0.05, indicating that the error difference is statistically significant. This result shows that by integrating the image texture features extracted by DINOv2 and the functional economic parameters, the model in this paper is more adaptable to carbon price fluctuations and improves the stability and robustness of cost prediction.

Optimized Material Selection and Cost Control Effect

To test the influence of different strategies on the selection effect of building materials in multi-objective optimization tasks, this section compares and analyzes the life cycle cost control ability and performance score of methods based on Bayesian Optimization (BO) and Differential Evolution (DE). The experiment selected five alternative solutions (Option 1–Option 5) with different trade-off configurations for key attributes such as lightness, thermal resistance, corrosion resistance, reflectivity, and flexibility, and recorded the dual response index cover results of each method in terms of cost and performance, as shown in Figure 5.

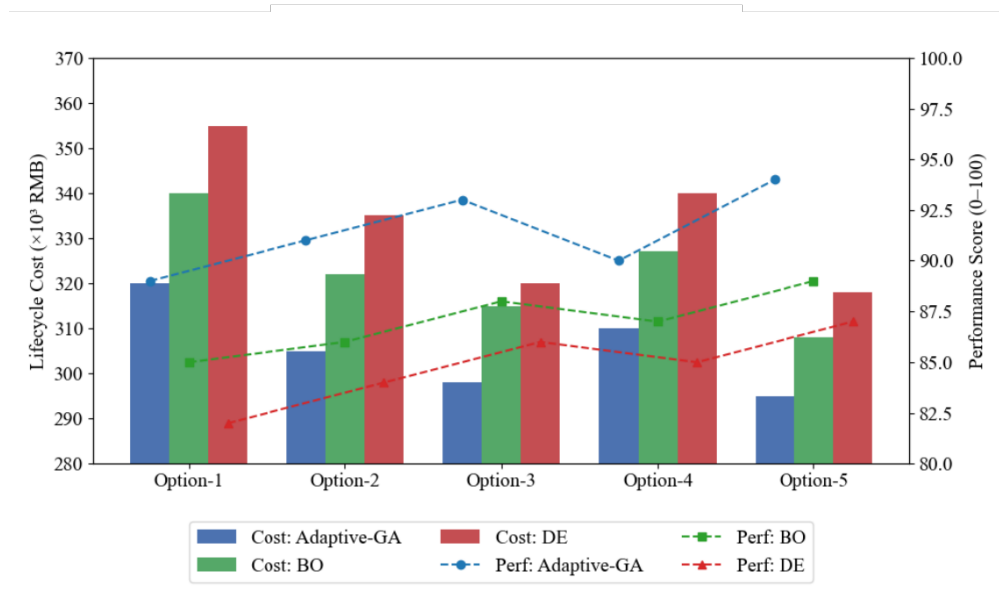


Figure 5. Comparison of life cycle cost and performance of architectural textile material selection

The five scenarios in Figure 5 (Options 1 through 5) represent different project priority settings, achieved by adjusting the weights between cost and performance in the optimization objective function. Option 1 prioritizes cost control, Option 5 prioritizes performance, and Options 2 through 4 are balanced strategies between the two. From the data, the algorithm in this paper achieves the highest performance of 94 points with the lowest cost of 295,000 CNY in Option 5, while the costs of BO and DE under the same option are 308,000 CNY and 318,000 CNY, respectively, and the performance scores are 89 and 87. Overall, Adaptive-GA can reduce costs and maintain or improve performance scores in most cases, while BO and DE generally have higher costs and slower performance growth. This difference stems from the mechanism characteristics of each algorithm in search strategy and model construction. Adaptive-GA uses adaptive genetic mechanisms to continuously adjust the selection, crossover, and mutation probabilities during population evolution, thereby reducing costs in the early stages and focusing on performance optimization in the later stages. BO relies more on the Bayesian model for global exploration. Although it is more robust in terms of balanced performance, its over-estimation of the sampling area may lead to insufficient resource allocation. In contrast, the DE algorithm is limited by its fixed parameters and broad search strategy, and the optimization path efficiency is not high, resulting in resource redundancy and cost increases.

Scalability and Applicability of the Method

This section analyzes the scalability and applicability of the method, focusing on the algorithm's performance when facing diverse material types and multi-scenario applications. First, this paper examines the convergence time of the algorithm as the number of material types gradually increases, and evaluates its ability to handle large-scale problems. All tests were conducted on the same experimental platform: an NVIDIA GeForce RTX 4070 GPU with an AMD Ryzen 7 5800X processor and 64 GB RAM. The convergence criterion is based on the fitness function's improvement threshold: if the optimal fitness value of the population does not improve by more than 0.5% over 20 consecutive generations, the evolution process is terminated. The maximum iteration round is capped at 200 to limit computation time. Subsequently, the generalization ability is compared based on the prediction error index in representative application scenarios to reflect its adaptability in actual complex environments. The corresponding results are shown in Figures 6 and 7.

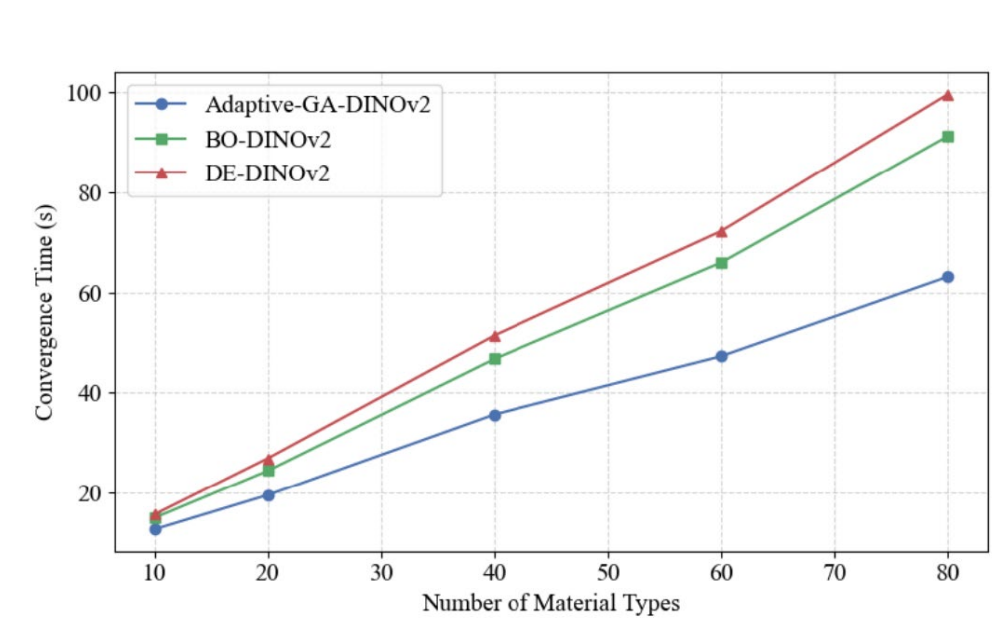


Figure 6. Scalability analysis of algorithm convergence time under multiple material types

Figure 6 shows that as the number of material types increases, the convergence time of the three algorithms increases, but the proposed method always demonstrates faster convergence. When there are 80 materials, the time is 63.1 seconds, which is better than BO-DINOV2 and DE-DINOV2, indicating that the algorithm has better scalability and efficiency in dealing with large-scale material selection problems. This advantage mainly

comes from the adaptive mutation rate mechanism introduced in this paper, combined with the rich texture features extracted by the DINOv2 model, which makes the optimization more accurate. In contrast, the BO and DE algorithms are less efficient in large-scale problems, and the convergence time increases, reflecting the lack of scalability.

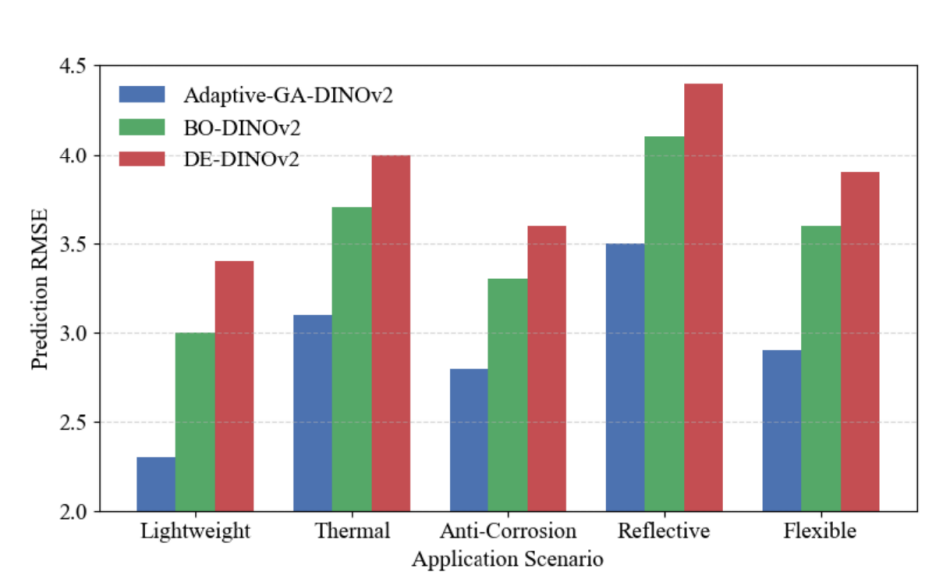


Figure 7. Comparison of algorithm prediction accuracy and applicability in different application scenarios

Figure 7 shows the root mean square error (RMSE) of the three algorithms in five application scenarios. The proposed method has the lowest error in all scenarios, with a minimum of 2.3 and a maximum of 3.5, which is significantly better than the BO and DE algorithms. BO and DE algorithms have errors of up to 4.1 to 4.4 in complex scenarios, indicating that their prediction performance is not stable enough. This difference stems from the in-depth extraction of local material features and the dynamic adjustment optimization strategy of the proposed method, which enables it to adapt to different functional requirements and ensures the generalization ability and applicability of the model. Relatively speaking, BO and DE lack flexibility and are difficult to cope with the diverse characteristics of complex materials, resulting in large prediction errors.

To evaluate the engineering applicability of this method, it was tested in three building application scenarios: low-energy residential envelope structures in extremely cold regions; curtain walls and sunshades for commercial buildings in hot summer and warm winter regions; and long-span flexible membrane structures for large stadiums. The RMSE of life cycle cost prediction and overall satisfaction rate were used as evaluation

metrics. The results are shown in Table 2.

Table 2. Performance Comparison of Different Algorithms in Building Application Scenarios

Algorithm	Scenario A: Low-Energy Residence		Scenario B: Commercial Building		Scenario C: Stadium	
	RMSE	Rate	RMSE	Rate	RMSE	Rate
	($\times 10^3$ CNY)	(%)	($\times 10^3$ CNY)	(%)	($\times 10^3$ CNY)	(%)
Adaptive-GA-DINOV2	3.12	89.86	2.95	90.03	3.24	83.59
BO-DINOV2	3.57	86.35	3.48	82.66	3.81	78.22
DE-DINOV2	3.86	85.21	3.72	81.98	4.23	75.34

Table 2 compares the performance of each method in three building application scenarios. Our method consistently achieves the lowest RMSE (2.95–3.24) and the highest satisfaction rate (83.59%–90.03%), demonstrating superior accuracy and robustness in satisfying various functional constraints compared to the baseline methods.

CONCLUSIONS

This paper proposes a method for intelligent selection and life cycle cost control of architectural textile materials that integrates the DINOV2 model. By introducing a local texture feature extraction module, the model's semantic recognition capabilities for complex textile materials are enhanced. A regression model combining functional and economic parameters is constructed to achieve cost quantification. An adaptive genetic algorithm is then employed for multi-objective optimization. Experimental results demonstrate that this method efficiently completes optimization, achieving a balance between low cost and high performance. The main contribution of this study lies in establishing an automated decision-making framework from visual recognition to cost optimization. However, practical applications still face challenges in acquiring and standardizing key data, as well as integration with existing BIM workflows. Future work will focus on building a standardized material database, developing interfaces with design software to promote practical application, and introducing a dynamic parameter mechanism to enhance the model's adaptability to market changes. Through further research and industry collaboration, this method is expected to become a practical intelligent

tool in green building design.

Author Contributions

All work in this study was independently completed by Hangtian Liu.

Conflicts of Interest

The author declares no conflict of interest.

Funding

This study was supported by the Key Project of the 2023 Shanxi Vocational Education Teaching "Research on the Construction of the '1+X' Certificate System" (Project No. 202302014).

Acknowledgements

Not applicable.

REFERENCES

- [1] Rubino C, Liuzzi S, Stefanizzi P, Martellotta F. Characterization of sustainable building materials obtained from textile waste: From laboratory prototypes to real-world manufacturing processes. *Journal of Cleaner Production*. 2023; 390:136098-136113. doi: 10.1016/j.jclepro.2023.136098
- [2] Ayed R, Bouadila S, Skouri S, Boquera L, Cabeza LF, Lazaar M. Recycling textile waste to enhance building thermal insulation and reduce carbon emissions: Experimentation and model-based dynamic assessment. *Buildings*. 2023; 13(2):535-557. doi: 10.3390/buildings13020535
- [3] Adriani NLPNC, Pranajaya IK, Suyoga IPG. Transformation and aesthetics of traditional Grinsing hand-woven textile: Textile motifs as decorative elements in modern interior design (A timeless beauty of modern artistry). *Law and Humanities Quarterly Reviews*. 2025; 4(1):101-110. doi: 10.31014/aior.1996.04.01.144
- [4] Segura Alcaraz MP, Bonet-Aracil M, Julia Sanchis E, Segura Alcaraz JG, Seguí IM. Textiles in architectural acoustic conditioning: A review. *The Journal of The Textile Institute*. 2022; 113(1):166-172. doi: 10.1080/00405000.2021.1976483

- [5] Pagnotta S, Filimon DI, Gallelo G, Lezzerini M. Building Material Recognition and Feature Extraction Using Small CCD Sensor and Image Analysis and Clustering Techniques. *Inżynieria Mineralna*. 2024; 1(1):229-236. doi: 10.29227/IM-2024-01-25
- [6] Dai M, Jurczyk J, Arbabi H, Mao R, Ward W, Mayfield M, et al. Component-level residential building material stock characterization using computer vision techniques. *Environmental Science & Technology*, 2024; 58(7):3224-3234. doi: 10.1021/acs.est.3c09207
- [7] Stergiou K, Ntakolia C, Varytis P, Koumoulos E, Karlsson P, Moustakidis S. Enhancing property prediction and process optimization in building materials through machine learning: A review. *Computational Materials Science*. 2023; 220:112031-112046. doi: 10.1016/j.commatsci.2023.112031
- [8] Zani A, Speroni A, Mainini AG, Zinzi M, Caldas L, Poli T. Customized shading solutions for complex building façades: The potential of an innovative cement-textile composite material through a performance-based generative design. *Construction Innovation*. 2023; 24(1):256-279. doi: 10.1108/CI-01-2023-0014
- [9] Neri M, Cuerva E, Levi E, Pujadas P, Müller E, Guardo A. Thermal, acoustic, and fire performance characterization of textile face mask waste for use as low-cost building insulation material. *Developments in the Built Environment*. 2023; 14:100164-100175. doi: 10.1016/j.dibe.2023.100164
- [10] Vėjelis S, Vaitkus S, Kremensas A, Kairytė A, Šeputytė-Jucikė J. Reuse of textile waste in the production of sound absorption boards. *Materials*. 2023; 16(5):1987-1999. doi: 10.3390/ma16051987
- [11] Dobilaitė V, Jucienė M, Bliūdžius R, Šveikauskaitė L. Investigation of some weathering impacts on tearing properties of PVC-coated fabrics used for architectural purposes. *Journal of Industrial Textiles*. 2022; 51(3_suppl):5328S-5346S. doi: 10.1177/1528083720982384
- [12] Priniotakis G, Marrot L, Stachewicz U, Krstic-Furundzic A, Venturini E, Jonaitiene V. Smart textile for building and living. *Autex Research Journal*. 2022; 22(4):493-496. doi: 10.2478/aut-2021-0041
- [13] Raghu D, Bucher MJJ, De Wolf C. Towards a 'resource cadastre' for a circular economy-urban-scale building material detection using street view imagery and computer vision. *Resources, Conservation and Recycling*. 2023; 198:107140-107151. doi: 10.1016/j.resconrec.2023.107140
- [14] Voronkov R, Bezuglyi M. Application of YOLO and U-Net models for building material identification on segmented images. *Informatyka, Automatyka, Pomiar w Gospodarce i Ochronie Środowiska*. 2025; 15(2):13-17. doi: 10.35784/iapgos.6968

- [15] Wang X, Han W, Mo S, Cai T, Gong Y, Li Y, et al. Transformer-based automated segmentation of recycling materials for semantic understanding in construction. *Automation in Construction*. 2023; 154:104983-104996. doi: 10.1016/j.autcon.2023.104983
- [16] Islam S, Bhat G, Mani S. Life cycle assessment of thermal insulation materials produced from waste textiles. *Journal of Material Cycles and Waste Management*. 2024; 26(2):1071-1085. doi: 10.1007/s10163-023-01882-7
- [17] Fonseca A, Ramalho E, Gouveia A, Henriques R, Figueiredo F, Nunes J. Systematic insights into a textile industry: Reviewing life cycle assessment and eco-design. *Sustainability*. 2023; 15(21):15267-15290. doi: 10.3390/su152115267
- [18] Altaf M, Alaloul WS, Musarat MA, Qureshi AH. Life cycle cost analysis (LCCA) of construction projects: Sustainability perspective. *Environment, Development and Sustainability*. 2023; 25(11):12071-12118. doi: 10.1007/s10668-022-02579-x
- [19] Yılmaz K, Aksu İÖ, Göçken M, Demirdelen T. Sustainable textile manufacturing with revolutionizing textile dyeing: Deep learning-based, for energy efficiency and environmental-impact reduction, pioneering green practices for a sustainable future. *Sustainability*. 2024; 16(18):8152-8175. doi: 10.3390/su16188152
- [20] Lee HS, Ha SH, Oh SH. Deep Learning Models for Fabric Image Defect Detection: Experiments with Transformer-based Image Segmentation Models. *The Journal of Information Systems*. 2023; 32(4):149-162. doi: 10.5859/KAIS.2023.32.4.149